Infiltration effects on a partially saturated slope - An application of the Discrete Element Method and its implementation in the open-source software YADE

Emanuele CATALANO

Thesis

Presented in partial fulfilment of the requirements for the degree of

Master Mécanique, Energétique et Ingénieries

Spécialité Modélisation et Expérimentation en Mécanique des Solides

Parcours international "Géomécanique, Génie Civil et Risques" (Geomechanics, Civil Engineering and Risks)

Université Joseph Fourier - Grenoble INP

June, 2008

Project Advisors:

    Frédéric DONZÉ   Professor, Université Joseph Fourier

    Bruno CHAREYRE   Maitre de conférences, Grenoble INP

    Luc SCHOLTÈS   PhD Student, Grenoble INP

Examiner at Home University:

    Giovanni BARLA   Politecnico di Torino, Italia

UNIVERSITE JOSEPH FOURIER
SCIENCES. TECHNOLOGIE. SANTÉ

Grenoble INP

Abstract

In this report, the collapse behaviour of a partially saturated granular slope is simulated using the Discrete Element Method (DEM), implemented in the open-source software YADE. The slope is considered as an assembly of spherical particules, whose interactions and motion are described respectively through a force-displacement law at the contacts and the application of the Newton's second law. The presence of water is taken into account at the microscopic scale, considering the existence of liquid bridges between the grains as it occurs in the pendular regime. The induced interparticle force can be computed through the capillary theory. At the macroscopic scale, these capillary forces result in an apparent cohesion and consequently, in a cohesive contribution to the stability, as described by the Mohr-Coulomb criterion. This contribution is discussed in terms of capillary stress effects on an unsaturated slope stability. Linking this capillary stress to the suction and degree of saturation, a suction profile can be defined along the slope height. As the water table position is defined from the suction distribution, infiltration phenomena are simulated by rising up its position through the slope height, resulting in a variation of the computed interparticle forces. The triggering of collapse by reduction of capillary stress is finally investigated.

Acknowledgements

Contents

INTRODUCTION

The analysis of slope stability constitutes one of the main subjects under developement in civil engineering. The need in predicting the movements of such large volumes of earth and preventing their destructive effects, when interacting with human settlements or activities, induced the developement of several analysis methods, which scope is to give an assessment of the slopes' tendency to be stable or rather to be susceptible of instability mechanisms.

The difficulties linked with the knowledge and the description of the mechanical behaviour of strongly heterogeneous materials encouraged mainly the developement of methods based on macroscopical approaches to the study of slope stability. In limit equilibrium methods (LEM) an assessment of the stability is provided through a factor of safety, defined as the ratio between strenght and induced forces along a pre-defined failure surface. Such a method results therefore to be more adaptable to probabilistic analyses, since the complex mechanisms of deformation that take place during instability phenomena are not taken into account in the analysis.

On the other hand, the developement of numerical tools to perform stability analysis met limitations due to too high computational time for simulations and the need of complex constitutive laws, which resulted in a weak interest in these approaches. In the last years, however, computers enhanced capacity allows the reduction in terms of time costs for simulations and encourages the exploitation of numerical methods implemented in modern calculators. They are based on different approaches, depending on the characteristics of the problem ([7]):

- The heterogeneous material is considered as a continuum, if it can be assumed that the medium behaves as a continuum and no localised discontinuities needs to be taken into account.

- It can be considered as an equivalent-continuum (classical in rock mechanics), whose properties are defined through macroscopic observations and assumptions, and by appropriate upscaling functions which relate the mechanical properties carried out by laboratory tests on samples (mesoscale) to the mechanical properties at the macroscopic scale, to reproduce its macroscopic behaviour.

- It can be finally considered as a discontinuum, following a microscopical approach, describing the material through the description of its solid phase, represented by interacting discrete elements, to reproduce the

macroscopic behaviour as a result of an appropriate micromechanical description of the deformation and motion phenomena.

In this work, the discontinuum approach is adopted to create a three dimensional model that would simulate the effects of infiltration in a partially saturated slope. The increase in water content results in a volume decrease, up to a condition that have been termed collapse. Research works conducted to collapse study of natural or artificial soils, revealed that the wetting-induced collapse is mainly due to the changes of the matric suction acting on the unsaturated soil structure ([11]). As the matric suction results from the capillary effects due to the formation of liquid bridges between couple of grains, inducing an attractive force between them, such a wetting-induced collapse is also considered to result from the changes in the capillary forces.

The main phases of the study are resumed in the following:

- The simulated material is characterized through triaxial tests performed on dry samples, opportunely prepared to realize a dense and a loose packing of particules. The mechanical suitability of the material is verified and the strenght parameters (friction angle) recovered (3.2.3);

- A scale factor is introduced, in order to relate the capillary forces computed for the virtual material, to forces that would come simulating any other granular material, characterized by the characteristic dimension of its grains. A validation obviously is proposed to justify its employement for the *SlopeStability* simulations (3.2.4);

- The Soil-Water characteristic curves are recovered for a sandy and a silty material, by subjecting the samples to wetting and drying processes. The respective maximum in cohesion is evaluated at low saturation degrees (3.2.4).

- A slope stability analysis is performed for a dry granular slope, submitted to the only gravity effects, to analyze the stabilization process, from the initial instable configuration, to the final quasi-static configuration (3.3.1);

- Slope stability analyses are then performed on wet slopes. A profile of matric suction is set along the slope height. Both the stabilization process and the effects of rising the water table are simulated, analyzing the effects of the water and comparing with the behaviour of the same material in dry conditions. The behaviour of a medium sized sand ($\Phi_{av} = 1mm$) and of a fine silt ($\Phi_{av} = 3\mu m$) are described (3.3.2)

4

All the simulations were run with the open-source sofware YADE. It has been developed in the laboratory 3S-R, thanks to the pioneer work by Donzé and Magnier ([6]) and the passion and dedition of all the Ph.D. students and professors who contribute daily to enhance its powerful, interpreting such an open-source philosophy and resulting in a free and constructive knowledge sharing.

Chapter 1

An insight into unsaturated soil mechanics

1.1 The matric suction theory

An unsaturated soil put in contact with free and pure water tends to soak up it due to presence of the total suction ψ. The total suction has two components: the matric suction S, which is associated to capillary phenomena, and the osmotic suction π, due to the presence of salts melt in the interstitial water and so to the difference of electro-chemical potential between the free and interstitial water.

$$\psi = S - \pi \qquad (1.1)$$

Often, dealing with unsaturated soils, geotechnical problems are related to changes in the only matric suction component. It will be seen in this work, how slope stability analysis can be performed considering changes in water content for a granular soil during prolonged rainfalls, neglecting the osmotic component whose variation is generally less significant during wetting processes [1].

1.2 Matric suction in natural conditions

The effects linked to the magnitude of the matric suction in a partially saturated soil are, as described before, directly linked to the capillary phenomenon. Classical experiments show how it occurs when the adhesive intermolecular forces between the liquid and a substance are stronger than the cohesive intermolecular forces inside the liquid. The effect causes a concave meniscus to form where the liquid is touching a surface. In unsaturated soils, voids constitute continous channels with variable section, along which
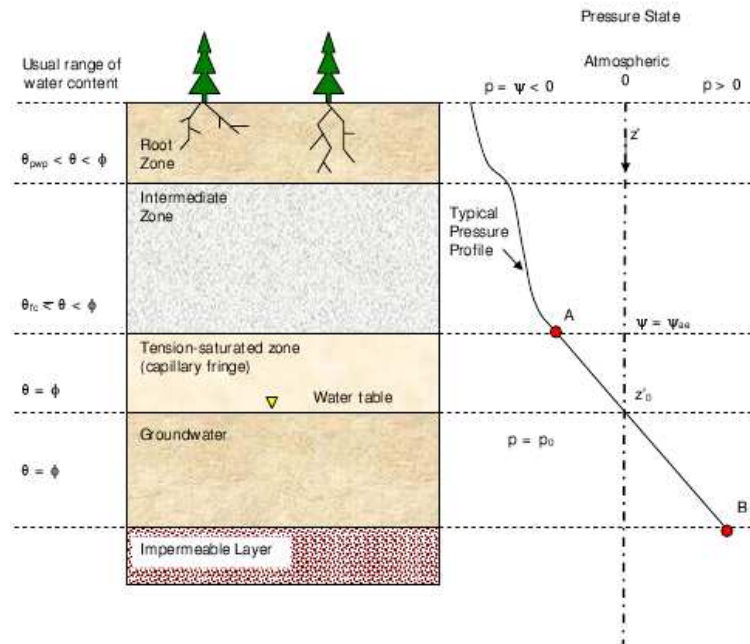
Figure 1.1: Schematized water content and pressure profiles

the water move from wet to dry zones, up to the capillary height, which depends on shape, dimension, granulometric distribution and arrangement of the soil particles. The concave shape of the meniscus created is due to the fact that the air pressure (atmospheric) is bigger than the water pressure u_w, from which it follows the negative sign of the matric suction, which, remembering Bishop, constitute an increment in effective stress and as a consequent to the total strength of the soil. In a partially saturated soil (fig.1.1), three zones can be recognized above the saturated zone, with different condition of saturation:

- A zone characterized by a very high degree of saturation ($Sr > 85\%$), the so-called **capillary zone**, where the gaseous phase (air or gas) is not continue but present in the form of air bubbles;

- The so-called **pendular zone**, characterized by very low saturation degrees ($Sr < 25\%$), where the liquid phase is not continue but present in the water menisci in correspondence of the interparticle contacts;

- A zone with intermediate degree of saturation, the **funicular zone**, where the two conditions just described coexist, and the liquid phase is more and more continue as the water content increases.

The zone of great interest for this work is the pendular one, where the presence of the water menisci and the discontinuity of the liquid phase realize a condition of compression between the grains at each interparticle contact. Because of the local capillary effects, the resultant apparent cohesion constitute a sensible contribution to the total strength available for the soil.

1.3   Phases of an unsaturated soil and proposed effective stress equations

A portion of a mixture can be considered as an independent phase, if it responds of both the following conditions: 1) differing properties from the contiguous material, and 2) definite bounding surfaces [1]. Unsaturated soils have usually been considered as a three-phase system - the water, the air and the particles of solid -, although some author proposed the introduction of a fourth phase, constituted by the air-water interface - or contractile skin -. This last assumption become important performing a stress analysis on an element, since from a behavioural standpoint, an unsaturated soil can be seen as a mixture with two phases that reaches the equilibrium under a defined gradient of stress - the solid particles and the contractile skin -, and other two phases that flow under applied stress gradient - the air and the water - [1]. It lends therefore support to the theoretical justification for using two independent stress state variables to describe the behaviour of unsaturated soils, without incorporating any soil parameter, therefore avoiding the difficulties due to the use of this kind of variables for the description of a stress state, which would depend on soil properties and on the specific problem to describe.

The first who recognized the separated effects of the total stress and pore-water pressure was M. A. Biot, the belgian physicist founder of the theory of poroelasticity, which in 1941 proposed an expression for the effective stress equation in the following form:

$$\sigma' = \sigma - \beta u_w \tag{1.2}$$

In 1959, Bishop suggested an expression for the effective stress principle, which has gained widespread reference:

$$\sigma' = (\sigma - u_a) + \chi (u_a - u_w) \tag{1.3}$$

where u_a is the air pressure, χ -the effective stress coefficient- is a parameter varying between 0 (dry material) and 1(saturated material). It's therefore a

constitutive property of the soil that depends on the actual degree of saturation and is furthermore linked to the stress path and the process to which the soil is subjected, which makes its assessment and use difficult. The term $(u_a - u_w)$ is called the matric suction, which is defined as the difference between the air and the water pressure. In an unsaturated soil the water molecules, in the proximity of the surface, are pulled inwards by other molecules deeper inside the liquid and are not attracted as intensely by the molecules in the neighbouring medium because of the absence of liquid over the surface itself. As a consequent, the free surface of such a soil behaves like a tense membrane which can resist to the so-called surface tension. In a partially saturated soil, the presence of such a surface tension, makes the water pressure smaller than the air pressure, and the matric suction negative, wherever above the water table.

1.4 The effective stress concept for saturated soils

The mechanical behaviour of a soil, its response under defined stress conditions, in terms of shear strength and strain, can be described in terms of state of stress in the soil. The stress variables need to be independent from the physical properties of the soil but rather to depend primarily upon the number of phases involved in each case. Therefore, it could be easily understood how the description of the behaviour of a saturated soil doesn't involve the same difficulties as in the case of partial saturation, and how the concept of effective stress needs more assumptions dealing with unsaturated soils.

The Terzaghi theory of consolidation established the concept of effective stress for saturated soils, expressed in the well known form:

$$\sigma' = \sigma - u_w \qquad (1.4)$$

where σ' is the effective stress, σ the total stress and u_w the pore-water pressure. The experimental evidence showed how this single stress variable was sufficient to described the behaviour of saturated soils, and the neutral influence of the pore-water pressure on the volume and shear strength change mechanisms.

1.5 Stress state variables for unsaturated soils

Considering the state of stress at a point in the soil, and performing an equilibrium stress analysis for an unsaturated soil, the stress variables controll-

9

ling the equilibrium of the soil structure can be recovered. The mechanical behaviour of a soil is assumed to be controlled by those variables. Three independent sets of normal stresses can be extracted from the equilibrium equation for the soil structure [1]. These are $(\sigma - u_a)$, $(u_a - u_w)$ and u_a, governing the equilibrium of the soil structure and the contractile skin. Assuming the soil particles and the water to be incompressible, the (u_a) variable can be eliminated and $(\sigma - u_a)$ and $(u_a - u_w)$ referred to as the stress state variables for an unsaturated soil. This combination comes form the choice of u_a as a reference, although other combinations are possible, this one appears to be the most adaptable to mostly engineering problems, since it allows to consider the separate effects of a change in total stress and in pore-water pressure, defining their magnitudes relqtive to the pore-air pressure, which correspond to the atmospheric pressure for most practical engineering problems.

1.6 Limiting Stress State Conditions - Slope Stability

Matric suction is closely related to environmental events that cause changing in the suction profile, along the depth in a soil, much more significant than any change in the net normal stress profile. The main factors that induce matric suction variations are [1]:

- The ground surface conditions, since the vulnerability to changes in suction profile are clearly function of the conditions of the ground surface, since a covered and protected surface would be less subjected to change in water content during precipitation events than an uncovered one;

- The environmental conditions, especially with seasonal changes, significant variations of the suction profile are registered, mainly near ground surface. Dry and wet season command therefore the magnitude of matric suction, closely linked to variations in water content in the soil;

- Important effects come from the presence of vegetation on ground surface and the beneficent effects of evapotranspiration processes, which result in removal water from the soil and an increase in matric suction;

- Being function of the degree of saturation at various depth, the matric suction magnitude is highly dependent on the position of the water table,

whose position become very important considering the effects on the matric suction near the ground surface;

- Finally the permeability of a soil, means its capacity to transmit and drain water, plays an important role in changes in matric suction as a result of environmental changes. Since it depends on the type of soil, different strata of a soil could affect in various manners the suction profile.

The stability of the equilibrium conditions is realized by the maintainement of a hierarchy with respect to the magnitude of the individual stress components in an unsaturated soil: $\sigma > u_a > u_w$ A clear example is available considering the air pressure momentarily increased in excess of the total stress, an "explosion" of the sample may occur. Any variation of the hierarchy expresses a limiting stress state condition. Therefore, imaging the pore-water pressure increasing in excess of the pore-air pressure, the degree of saturation would approach 100% and the matric suction goes to zero. The behaviour of the soil would be now described in terms of one stress state variable, $(\sigma - u_w)$. By these considerations, the phenomenon of liquefaction can be described as the reach of a limiting condition when the pore-pressure water increase and the stress variable $(\sigma - u_w)$ reaches zero.

Chapter 2

The Discrete Element Method and Yade

2.1 Introduction

"The discrete element method is a numerical tool capable of describing the mechanical behaviour of assemblies of discs or spheres. The method is based on the use of an explicit numerical scheme in which the interaction of the particles is monitored contact by contact and the motion of the particle modelled particle by particle [...]" (Cundall and Struck, 1979). This exhaustive definition, by the abstract of the work by Cundall and Strack (1979) [5], introduces the main aspects of the model, and suggests the powerful of its implementations, with the development in two and three dimensions of codes able to simulate the mechanical behaviour of granular media. In this section the Discrete Element Method (DEM) will be presented in a short way and its the modern implementations in modern codes, as YADE (Yet Another Dynamic Engine), the code used in this work to simulate the behaviour of a partially saturated granular slope, initially introduced by Donzé and Magnier [6], and recently enhanced to take into account the capillary effects at contacts and their consequences in termes of attractive forces between grains and water retention.

2.2 The Discrete Element Method and the YADE code

The Discrete Element Method allows the definition of the mechanical laws of interaction and deformation of contacting particles, and simulates the macro-
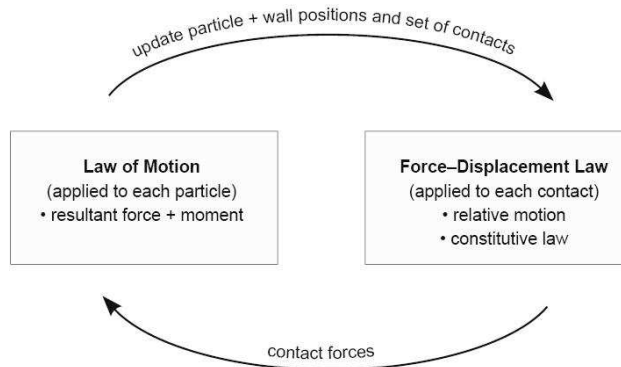
Figure 2.1: The calculation cycle

scopic response of the assembly as function of a given external load. The treatment of its principal aspects will focus on spherical particles, available for 3D simulations in YADE ([16], [15]), and able to show in an appreciable way the macroscopic behaviour of the granular matter. Each sphere is identified in the model by its own mass m, radius R and moment of inertia I_0.

The calculations alternate between the application of Newton's second law to the particles and a force-displacement law at the contacts. Newton's second law is used to determine the motion of each particle arising from the contact and body forces acting upon it, while the force-displacement law is used to update the contact forces arising from the relative motion at each contact.

The calculation cycle is therefore a timestepping algorithm that requires the repeated application of the law of motion to each particle, a force-displacement law to each contact, and a constant updating of wall positions. Contacts, which may exist between two balls or between a ball and a wall, are formed and broken automatically during the course of a simulation. At the start of each timestep, the set of contacts is updated from the known particle and wall positions. The force-displacement law is then applied to each contact to update the contact forces based on the relative motion between the two entities at the contact and the contact constitutive model. Next, the law of motion is applied to each particle to update its velocity and position based on the resultant force and moment arising from the contact forces and any body forces acting on the particle. Also the wall positions are updated based on the specified wall velocities. The process of calculation is represented in fig.2.1.
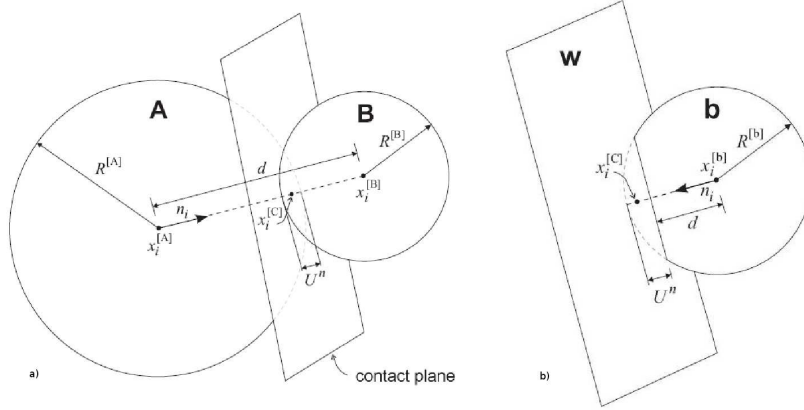
Figure 2.2: Geometry of interactions. a) Sphere-sphere contact. b) Wall-Sphere contact.

2.2.1 The Force-Displacement Law

The force-displacement relates the relative displacement between two entities at a contact to the contact force acting on the entities and occurring at a point. In partially saturated soils, an additional attractive force can also act on each particle, resulting from the presence of the water which forms, for low saturation degrees, liquid bridges bonding each other the particles. The contribution of this force will be detailed later. Other forces and moments could derive by considering other phenomena like the cementation due to solute precipitation. Focusing on the contact effects, the force-displacement law can be described in terms of a contact point (fig.2.2), defined by the vector $x_i^{[C]}$, lying on contact plane that is defined by its unit normal vector n_i, linking the two centers in ball-ball contacts, and standing on the shortest distance line in ball-wall contacts. The two components of the force acting on the contact plane are related to the corresponding two components of displacement through a normal and a shear stiffness at the contact.

The contact ball-ball will be described in some detail. The overlap U_n, defined to be the relative contact displacement in the normal direction, and the contact point position $x_i^{[C]}$ are computed as function of the radius $R[\Phi]$ and the position of the centers of the two spheres Φ. The resultant force can be resolved into its normal component and shear component:

$$F_i = F_i^n + F_i^s \tag{2.1}$$

The normal contact force is calculated by:

$$F_i^n = K^n U^n n_i \tag{2.2}$$

14

where K^n is the normal stiffness defined at the contact. It becomes necessary here to give some description on how stiffnesses are defined in the model. They are computed on the base of an homogeneization formula. The normal stiffness K^n is a secant modulus that relates total displacement and force. It is computed as function of the interacting particle dimensions R_Φ and of a global charactristic modulus of the material E, resulting in a constant ratio between E and the effective bulk modulus of the packing, whatever the size of the particles.

$$K_n = \frac{2ER_1R_2}{R1 + R2} \tag{2.3}$$

On the other hand, the shear stiffness K^s is a tangent modulus - $k^s = \alpha K_n$ - relating incremental displacement and force. The shear component of the resultant force is computed as function of the relative tangent displacement d_t, it is therefore initialized to zero and then updated considering each relative shear-displacement increment which results in an increment of the elastic shear force. The motion of the contact is considered in the procedure, to update the two vectors n_i and $x_i^{[C]}$ at each timestep. The incremental force is then computed by the following expression:

$$\Delta F_i^s = -k^s \Delta U_i^s \tag{2.4}$$

where ΔU_i^s is the contact displacement-incremental vector, computed for a timestep Δt as a function of the shear component of the contact velocity. As purely friction materials are used in YADE, the strenght of contacts is defined by the Coulomb friction law:

$$|f_s| \leq f_n tan\,(\phi_s) \tag{2.5}$$

where μ_s is the intergranular friction angle. The whole computation procedure is shown in fig.2.1.

2.2.2 Law of motion

Spherical particles are used in this work to simulate the behaviour of a granular medium. Each sphere, at each timestep, is characterized by its position x_i, velocity $\dot{x}_i$ and acceleration $\ddot{x}_i$, defining its translational motion and by its angular velocity ω_i and angular acceleration $\dot{\omega}_i$, defining the rotational motion. Forces and moments acting on the particle are computed as described in the previous section. The equations of motion can be expressed as two vector equations:

- The equation for the translational motion:

$$F_i = m \left(\ddot{x}_i - g_i \right) \tag{2.6}$$

  where F_i is the resultant force acting on the particle, m its total mass, g_i the body force acceleration vector;

- The equation for rotational motion:

$$M_i = I \dot{\omega}_i \tag{2.7}$$

  where I indicates the moment of inertia of the particle and M_i the resultant moment acting on it.

The equations of motions are integrated using a centered finite-difference procedure involving a timestep of Δt, as described by the following expressions.

$$\ddot{x}_i^{(t)} = \frac{1}{\Delta t} \left(\dot{x}_i^{t+\Delta t/2} - \dot{x}_i^{t-\Delta t/2} \right) \tag{2.8}$$

$$\ddot{\omega}_i^{(t)} = \frac{1}{\Delta t} \left(\dot{\omega}_i^{t+\Delta t/2} - \dot{\omega}_i^{t-\Delta t/2} \right) \tag{2.9}$$

These expressions enter into the computation of $\dot{x}_i$ and ω_i, at the mid-intervals $t \pm \Delta t/2$.

$$\dot{x}_i^{(t+\Delta t/2)} = \dot{x}_i^{t-\Delta t/2} + \left(\frac{F_i^t}{m} + g_i \right) \Delta t \tag{2.10}$$

$$\dot{\omega}_i^{(t+\Delta t/2)} = \dot{\omega}_i^{t-\Delta t/2} + \left(\frac{M_i^t}{I} \right) \Delta t \tag{2.11}$$

The velocities computed allow the update of the positions of the particle centers, for the time $t + \Delta t$. The forces and moments are then computed by the application of the force-displacement law (eq.2.2, 2.4.

2.2.3 Convergence conditions

As the solution scheme is based on the discretization of time, the convergence to a stable solution depends on the time step Δt, which need to be limited. Studying the vibrations of a system using a centered finite-difference procedure, from the condition of stability of the solution for a given perturbation imposed to the problema a critical time step is defined, which is function of the natural period of the system. Here the natural period of each particle is calculated, computed at each contact by an equivalent stiffness K computed

for all the i degrees of freedom, supposed independent. The critical time step is finally computed as a fraction S of the minimum natural period computed.

$$\Delta t_{crit} = S \cdot min \left(\sqrt{m/K} \right) \tag{2.12}$$

where m/K is computed for each degree of freedom and elements in contact.

2.3   Unsaturated soil framework

Macroscopic properties of granular materials such as soils depend mainly on the interactions between the particles at the microscopic level. Modelling dry granular material by a micro-mechanical approach, the internal particle forces coming from each interaction are related to the applied external loads, as it has already been investigated [9]. Dealing with unsaturated soils, some assumptions are needed in order to take into account the presence of water. Indeed, as described in the previous chapter, its consequences in terms of forces and water retention have to be considered at the microscopic level, especially near the ground surface. The presence of the water leads to the formation of water menisci between neighbouring grains, as a result of in-filtration, evaporation or capillary phenomena. These menisci result in new interparticle forces, which are highly dependent on the degree of saturation, as one could suppose considering the two limit states, the dry one (Sr=0%) and the saturated one (Sr=100%). Along the profile of an unsaturated soil, the water is present in different configurations, and needs therefore different assumptions for its distribution from the water table to the ground surface. For low water contents, near the ground surface, the water is supposed to form liquid bridges between neighbouring grains, which don't constitute a continuous liquid phase (pendular regime). Capillary theory allows the forces induced by those bridges to be linked to the local geometry of the interaction and to the matric suction in the medium [2]. The increase in water content with the depth results in the progressive fusion of the liquid bridges (see fig.2.3) and the consequent annulation of attractive forces between grains, up to the condition of complete saturation corresponding to the water table, where, as expressed by the Terzaghi formulation for the effective stress, and experimentally confirmed, the water effects become neutral in volume and shear strength change mechanisms.

Here the micromechanical interpretation for the pendular regime will be presented, as it has been analyzed [3] and implemented in YADE.
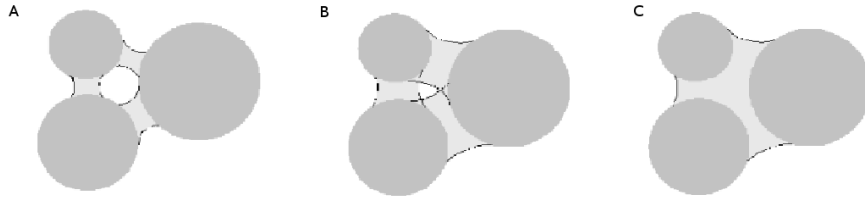
Figure 2.3: The evolution of the water bridges during a wetting process. Pendular regime (A). Funicular regime (B). Saturated regime (C).
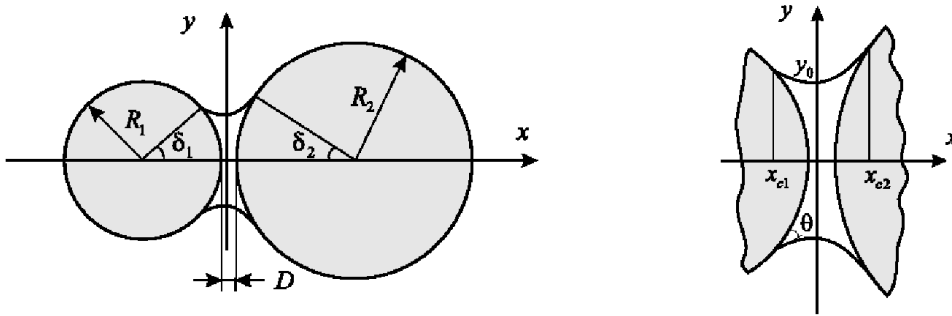

Figure 2.4: Geometry of liquid bridges in the pendular regime of an unsaturated soil

2.3.1 Micromechanical interpretation of the pendular regime

In the pendular regime, characterized by low degree of saturation ($Sr <$ 25%), each liquid bridge is assumed to connect only two particles, and to be responsible of an attractive force in between them. At the macroscopic level that results in a positive contribution to the effective stress, therefore straightforward in an increment of the shear strenght of the soil (see next section). Anyway, dry contacts can persist, depending on the water content and the texture of the medium. Therefore, under these conditions, two kind of forces coexist in the medium, a repulsive force due to contact and an attractive force resulting from water bridges effects. Repulsive forces resulting from dry contacts are detailed in the previous section. Here focus is put on the forces arising from the presence of liquid bonds between particles, consequence of the interface action between air and water. The shape of the liquid bonds connecting spherical particles is fully described by the Laplace equation, which allow the computation of the mean curvature C of the liquid bridge and the surface tension γ of the liquid phase, as function of the matric

18

suction $(u_a - u_w)$:

$$S = \Delta u = \gamma C = \gamma \left(\frac{1}{r_1} + \frac{1}{r_2} \right) \tag{2.13}$$

Considering the geometrical description of the liquid bridge (fig.2.4), the intergranular force F^{cap} and the water volume V_m can be computed as functions of the distance D and capillary pressure Δu. The resulting suction controlled model allows therefore to associate a force and a water volume to each interacting grain of an assembly [3].

$$\left(F^{cap}, V_m \right) = \Lambda \left(\Delta u; D \right) \tag{2.14}$$

The interparticle force F_{cap} induced by both the liquid surface tension and the matric suction can be calculated at the profile apex y_0 of the bridge (fig.2.4) following the gorge method [3]:

$$F^{cap} = 2\pi y_0 \gamma + \pi y_0^2 \Delta u \tag{2.15}$$

The water is taken into account by its presence in menisci bonding couple of grains. No adsorbed or residual water are considered. Therefore the volume of water (eq.2.16), self-distributed homogeneously in the sample, is simply computed as the sum of all the menisci volumes, and the degree of saturation S_r can be assessed by summing all the menisci volumes (eq.2.17).

$$V_m = \pi \int_{x_1}^{x_2} y^2(x)dx - \frac{1}{3}\pi R_1^3(1 - acos(x_1))^2(2 + acos(x_1)) \\ - \frac{1}{3}\pi R_2^3(1 - acos(x_2))^2(2 + acos(x_2)) \tag{2.16}$$

$$Sr = \frac{\sum_{m=1}^{N_m} V_m}{V_v} \tag{2.17}$$

In the figure 2.5 a schematic representation shows the resulting interaction force as a function of D, introducing. The choice is made to allow the formation of the bridges when particles come strictly in contact ($D_{creation} = 0$), whereas its rupture $D_{rupture}$ depends on the defined capillary pressure and on the local geometry. The rupture of the bridge corresponds to the value for which the Laplace equation does not provide a stable configuration of the liquid bridge.

2.4 Stress considerations for partially saturated soils

As described before, the presence of water leads, in the pendular regime, to the formation of liquid bridges between coupled of grains. This results in an
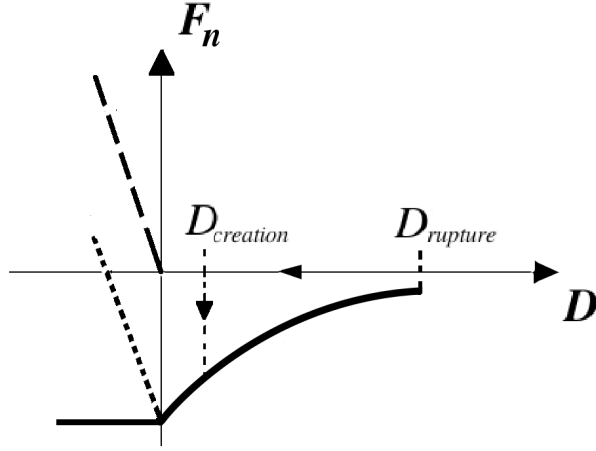
Figure 2.5: Behaviour of the capillary law as a function of the interparticle distance D for a given capillary pressure (solid line). The elastic repulsive normal force resulting from an overlap ($D < 0$) is shown in the long-dashed line, and the resultant normal force in this range is shown by the short-dashed line. Capillary force as function of the intergranular distance D

additional attractive force, which is assumed to be a function of the capillary pressure and of the geometry of the interaction. By the homogeneization technique, assumptions done at the microscopic scale are reported at the macroscale. The Love static homogeneization is used, in order to express the mean stress tensor $\bar{\sigma}$ within a volume of granular matter V as a function of the external forces $\vec{F}^{ext,p}$, of whatever nature, applied to particles p belonging to the boundary volume ∂V:

$$\sigma_{ij} = \frac{1}{V} \sum_{p \in \partial V} F_i^{ext,p} x_j^p \tag{2.18}$$

where $\vec{x}^p$ is the coordinate of the particle p with respect to a suitable frame. Considering the mechanical balance of each particle of the volume V equation, we can write:

$$\sigma_{ij} = \frac{1}{V} \sum_{p=1}^{N} \sum_{q=1}^{N} F_i^{q,p} l_j^{q,p} \tag{2.19}$$

where N is the number of particles within the volume, $F_i^{q,p}$ is the interaction force exerted by the particle q onto the particle p, and $l_j^{q,p}$ the branch vector pointing from the particle q to the particle p. As precised before, when dealing with partially saturated soils, two kind of interaction forces can be

distinguished, a contact force $\vec{F}_{cont}^{q,p}$ and a capillary force $\vec{F}_{cap}^{q,p}$. Both the forces can coexist, depending on the geometrical properties of the interacting spheres, so we can write:

$$\vec{F}^{q,p} = \vec{F}_{cont}^{q,p} + \vec{F}_{cap}^{q,p} \tag{2.20}$$

for any couple of spheres $(p, q) \in [1, N]^2$.

The straighforward consequence in terms of stress is recoverable combining (2.19), (2.20).The stress tensor is split in two components,

$$\sigma_{i,j} = \sigma_{ij}^{cont} + \sigma_{ij}^{cap} = \frac{1}{V} \sum_{p=1}^{N} \sum_{q=1}^{N} F_{cont}^{q,p} l_j^{q,p} + \frac{1}{V} \sum_{p=1}^{N} \sum_{q=1}^{N} F_{cap}^{q,p} l_j^{q,p} \tag{2.21}$$

σ_{ij}^{cont} arising from the contact forces, and σ_{ij}^{cap} from the capillary ones.

2.5 Triaxial tests in unsaturated conditions

Here, the effects of capillary water in DEM experiments are described through data coming from triaxial tests performed on unsaturated granular assemblies [3]. Adopting an increasing value in matric suction, the straight line corresponding to the Mohr-Coulomb failure criterion is recovered (2.22), and all the mechanical parameters of the material can be evaluated through:

$$\tau = c_{app} + \sigma tan(\phi) \tag{2.22}$$

In fig.2.6a results of the first session tests are reported, for saturation degrees varying between 0.01% and 10%. The peak in deviatoric stress is found, as expected, to be greater for unsaturated materials, and to depend on the the saturation degree, whereas the volumetric strain more contractant(2.6b). For the other tests performed for different value of confining stress(see fig.2.5a, results in the $q - p$ plane show how the friction angle is independent of the matric suction value, and results the same for any level of saturation. It is also worth noticing how the value of the cohesion can be considered equivalent to the trace of the capillary stress tensor (see fig.2.5b); in the following the cohesion will be quantitatively evaluated through this quantity.
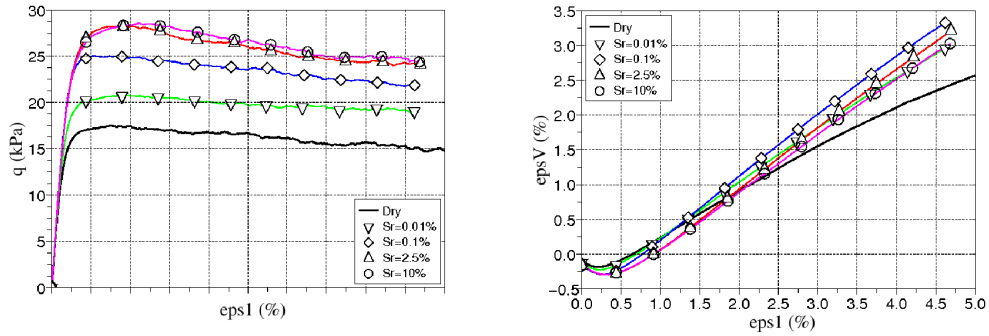
Figure 2.6: Deviatoric stress versus axial strain for triaxial tests in unsaturated conditions (a). Volumetric versus axial strain (b)
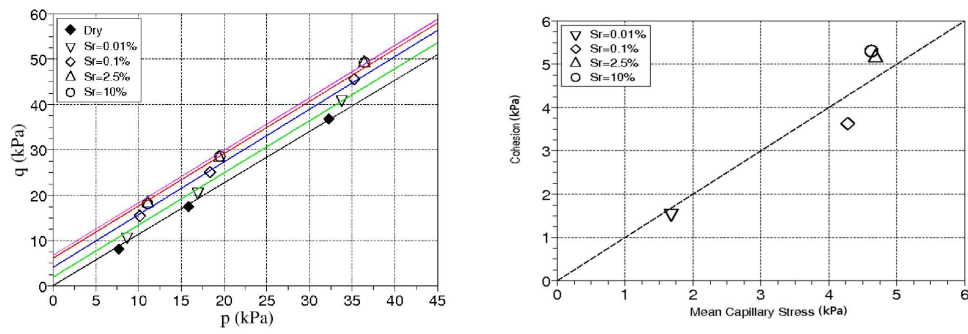

Figure 2.7: Data from triaxial tests performed on unsaturated samples for various saturation degrees (a). Cohesion versus the capillary stress tensor trace (b).

Chapter 3

Slope stability analysis of a granular slope

3.1 Introduction

The open-source software YADE had been used to simulate the behaviour of a partially saturated slope. The code, as described in the previous chapter, has been recently enhanced to take into account the capillary effects which characterize unsaturated soils. This function constitutes with many others the "motors" of YADE, called *"engines"*, that allow the user to create and develop his own application, in order to perform simulations by defining all its properties and logical operations. The scope of this work is the development of the *SlopeStability* application, which would allow the simulation of instabilities due to a change in water content in a slope. Based on the work of Griffiths and Lu ([10]), where a slope stability analysis is performed by using elasto-plastic finite elements, the schematized slope is defined to ensure a proportion of 1 x 1/3 x 1/3 of its xyz dimensions (fig.3.1). A profile of matric suction can be also defined as input in the model. For the sake of
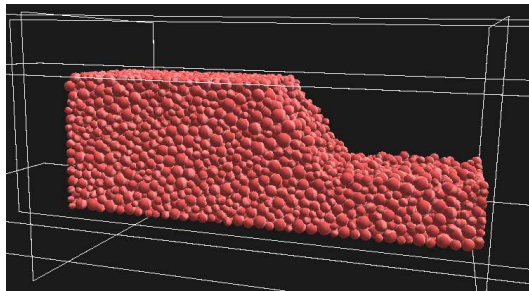

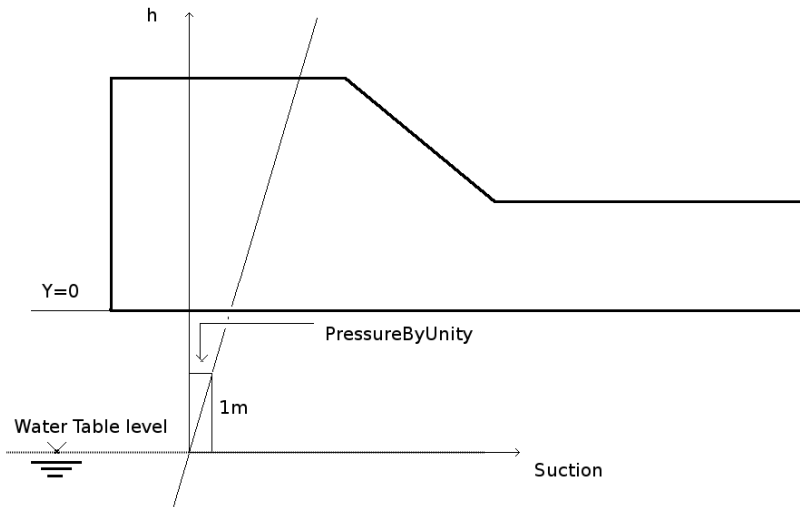Figure 3.1: Simplified geometry of a granular slope.

Figure 3.2: Suction profile

simplicity, a linear profile for the matric suction is adopted, fully defined by a unique parameter which define the value of negative pressure for a unity of depth of the soil, above the water table, where the capillary pressure is assumed to be null. This parameter is taken to be equal to the volumetric weight of water, ensuring the capillary pressure to increase by 10000 Pa by meter above the water table (see fig.3.2.

Suction profiles are in reality more complex (see 1.2), sensible to seasonal changes, strongly influenced by the ground conditions. The linear distribution can be an acceptable assumption in order to evaluate the contribution of the cohesion, which is a direct consequence of the existence of capillary forces inside the medium, the aim of the work being related to the study of capillary effects annulation with increasing water content

3.2 The testing program for DEM experiments

3.2.1 Triaxial testing

The material used in DEM experiments is fully characterized by triaxial tests on cubic samples. The homogeneity of the loading over the sample is assured through frictionless boundary walls, which avoid any unwanted boundary effect. The behaviour of geomaterials is usually described by time-independent laws. In order to be able to assess the magnitude of such time-independent charateristics of a geomaterial by performing triaxial tests, it is necessary to

assure an appropriate loading rate. That is exactly what it's expected by a numerical model of a triaxial test, where the strain rate is controlled in order to ensure a quasi-static equilibrium between the internal stress σ_{int}, corresponding to the homogeneized stress resulting from interaction forces (see eq.2.18), and the external stress σ_{ext}, which results from the resultant forces at the boundary. As the simulations result from a dynamical process (solving Newtons law), quasi-static equilibrium is assured by controlling the loading rate so as the normalized mean resultant force on particles (which is 0 at static equilibrium) does not exceed 1% of the mean contact force at each loading step. This "stability indicator", called in the following $UnbalancedForce$, is controlled by fixing an appropriate value of the strain rate during the simulations, providing that smaller values don't involve any change in the response. Dry samples were used to set the parameters of the model. The friction value characterizing the material is found out directly on Mohr circles representations of the stress state.

3.2.2   Scaling the particle size distribution

The characterization of the simulated material is important to verify its behaviour under loading to be mechanically suitable. Anyway, in order to be able to simulate the behaviour of any granular materials, being not possible to deal with the real dimensions of the grains because of the limitation in the number of particles which can be set for a simulation, an appropriate scale factor is introduced, which depends on the average diameter of the granular assembly one wants to consider in his analysis. This scale factor, labelled α, is calculated with the equation 3.1,

$$R^R = \alpha R_Y \tag{3.1}$$

where R^R is the radius of the real material and R_Y is the average radius of the sample created with YADE. The scale factor acts only on the capillary forces, since for dry samples to considering different grain dimensions corresponds in a change of weight for all the particles but does not involve any change in macroscopic behaviour of the assembly [4]. Dealing with unsaturated samples and seeing how capillary forces are strictly dependent on the geometry of the liquid bridge between the grains, involve a need in scaling the capillary forces, which otherwise would be negligible with respect to the weight of the particules. The scale factor acts therefore on grain sizes, in order to scale the geometry of the liquid bridge configuration to the new dimensions considered. The introduction of such a parameter needs to be validated through the suitability of its effects. This is seen in 3.2.4.
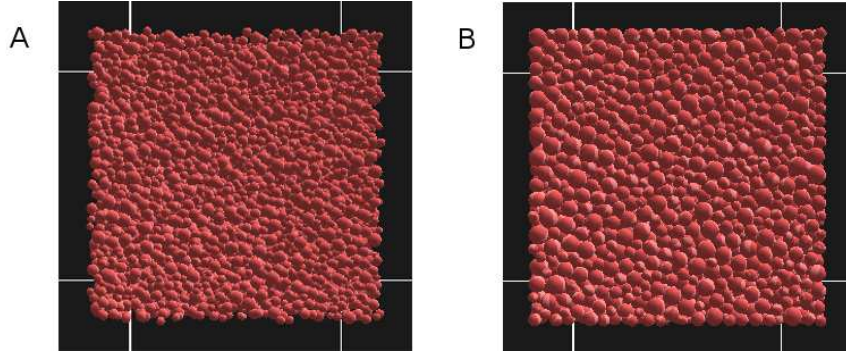
Figure 3.3: Preparation of the samples. A.Uncompacted sample. B.Compacted sample

3.2.3 Triaxial tests in dry conditions

The DEM numerical samples are polydisperse assemblies composed of 10000 spheres. A dense and a loose sample were prepared, in order to verify the expected differences in response under loading, in terms of volume variations and deformations. The preparation of a sample consists in its compaction under a defined isotropic state of stress, realized by increasing the particle radii over the sample, the walls remaining fixed and frictionless. The magnitude of the forces coming from interactions at each spheres contact depend on the radii growth, which stops once the resultant force on the walls is equivalent to the chosen confining stress (fig.3.3). Different porosities can be otained for a sample, managing the friction angle that characterize the interactions, during compaction phase. In our simulations a very small value of friction angle (0.5°) was set to obtain a dense sample, whereas an angle of 20° was chosen to simulate a loose one. The relative porosities are equal to 0.39 and 0.42 respectively. Both the samples are characterized by a grain size distribution ranging between 0.35mm and 0.7mm. The confining pressure was set to 5kPa to perform the triaxial tests. Table 3.2.3 resume the main input parameters adopted for the simulations. For the dense sample (see fig. 3.4), a

Global Modulus E (MPa)	k^s/K_n α	Friction angle ϕ (deg.)	Strain Rate $\dot{\varepsilon}$	σ_{iso} [Pa]
50	0.5	30	0.5	5000

Table 3.1: DEM model parameters

strain softening behaviour is observed, associated with dilatancy. A peak in
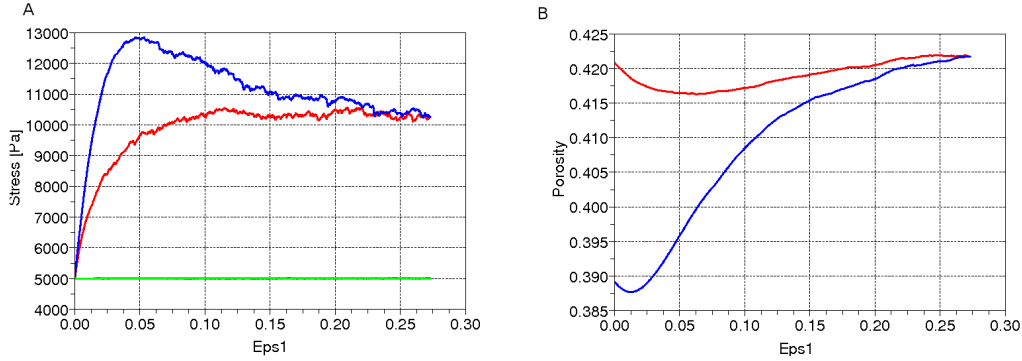
26

Figure 3.4: Axial compressive stress and porosity versus axial strain obtained from triaxial tests in dry conditions for a dense (A) and for a loose (B) sample.

the stress-strain curve is detected. For the loose sample a mainly contractant behaviour is observed, followed by a smooth dilatancy and positive volumetric strains for high levels of deformation (20% axial strain). The stress-strain curves for the dense and the loose sample converge both to an equivalent asymptotic value at the critical state, confirming the mechanical suitability of the simulated material. The Mohr circles are traced (see fig.3.5), corresponding to the peak and the residual level of stresses. The values of friction angles are carried out, being 26° at the peak and 22° the residual one.

3.2.4   Soil-Water Characteristic Curves

In this section, unsaturated samples are subjected to wetting and drying cycles, in order to evaluate the relation between the water content in the soil and the matric suction. The evolution in terms of cohesion, straightforward linked to the magnitude of the capillary pressure and the degree of saturation in the soil, can be recovered thanks to the function which detects the fusion of menisci as a result of the increase in water content. The geometry of bridges had been clearly described in previous sections. The fusion of menisci is detected through geometrical considerations that provide a critical condition for the existence or the permanence of the bridge. In YADE, once the bridges are touching each others, the liquid phase can no more be considered as discontinue (2.3). As suggested by Jang [12] the choice was made to remove each capillary force associated with fusioned menisci. This results in a decrease of the cohesion and, numerically, in the simulation of the wetting process. It's clear how the hypothesis done in the funicular and in the capillary regimes of the unsaturated soil, is done in order to provide a compatible behaviour of the capillary effects on the cohesion during a wetting process,
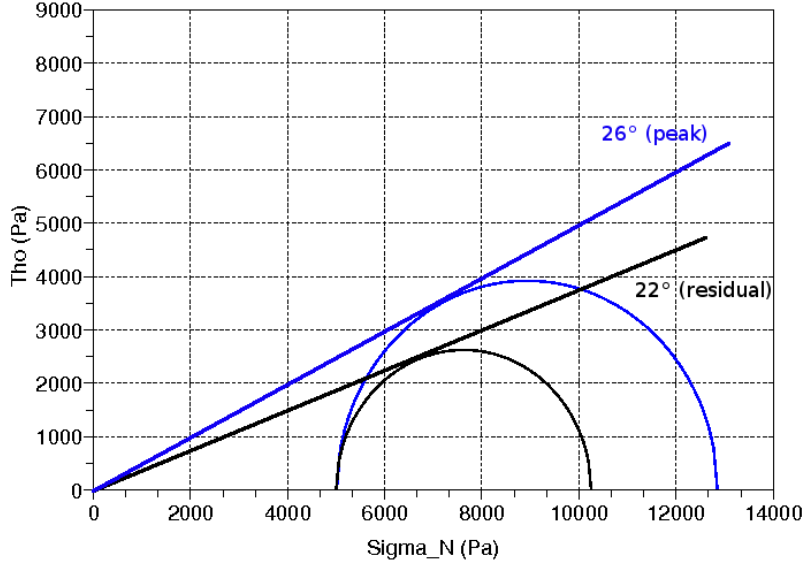
Figure 3.5: Mohr circles representation of the dry triaxial tests. Peak (blu) and residual (black) conditions.

but would need obviously an additional micromechanical interpretation for the forces effectively acting on the particles of soil.

A first session of simulations was performed in order to validate the introduction of the scale factor α, necessary to simulate the behaviour of real geomaterials, as described in 3.2.1, obviously under the same hypothesis of homogeneity. As described in 3.2.2, this factor is introduced to scale the capillary forces computed by using the simulated material, to the *real* capillary forces. The computation of the capillary stress tensor, as it is defined in (2.21), is recalled:

$$\sigma^{cap,Y} = \frac{1}{V} \sum_{p=1}^{N} \sum_{q=1}^{N} F_{cap,Y}^{q,p} l_{j,Y}^{q,p} \tag{3.2}$$

where Y indicates we are dealing with the simulated material. Through the introduction of the scale factor, the equivalence between the capillary stress computed with the simulated material and the capillary stress of the real material, $\sigma^{cap,REAL}$, has to be ensured. This results straightforward from the introduction of the scale factor, defined as in eq.3.1, in the computation of

28

the capillary stress tensor:

$$\sigma^{cap,Y} = \frac{1}{V\alpha^3} \sum_{p=1}^{N} \sum_{q=1}^{N} F_{cap,Y}^{q,p} \alpha l_{j,Y}^{q,p} \tag{3.3}$$

Being the real capillary stress tensor, computed as,

$$\sigma^{cap,REAL} = \frac{1}{V} \sum_{p=1}^{N} \sum_{q=1}^{N} F_{cap,REAL}^{q,p} l_{j}^{q,p} \tag{3.4}$$

the equivalence between the two formulations comes by computing:

$$F_{cap,REAL} = F_{cap,Y}/\alpha^2 \tag{3.5}$$

Here the behaviour of a sand is simulated, considering an average value for the diameter of 1mm (see fig. 3.6). To validate the scaling assumption, two cubic samples of different volume ($l_1^3 < l_2^3$) were used, whose average radii allowed the definition of two scale factors, α_1 and α_2. Table 3.2.4 resume the main parameters of the simulations.

Φ_{av}^1 [mm]	Φ_{av}^2 [mm]	$\Phi_{sand,av}$ [mm]	α_1 [mm]	α_2 [mm]
0.30	0.45	1	3.33	2.22

Table 3.2: Scale factors α

The two samples were both subjected to a wetting process. An initial high value of capillary pressure S (400000 Pa) was set, homogeneously distributed over the sample, and decreased at each iteration of a fixed value dS. The subsequent increase in water content is simulated and its effects on the mean capillary stress evaluated, through the calcualtion of the trace of the capillary tensor. The resulting data (see fig.3.7) validate the effect of the scale factors $\alpha_{1,2}$ on the computation of the capillary forces and on the resultant capillary stresses. The same material can be suitably simulated with any granular assembly so as the scale factor α is well defined. It can be observed how the mean capillary stress doesn't reach high values as a result of the presence of menisci between grains. This can be considered as an expected result for a sand whose characteristic dimensions do not involve high levels of cohesion which, as it will be clear later performing slope stability analysis, remain less significant than the gravity effects.
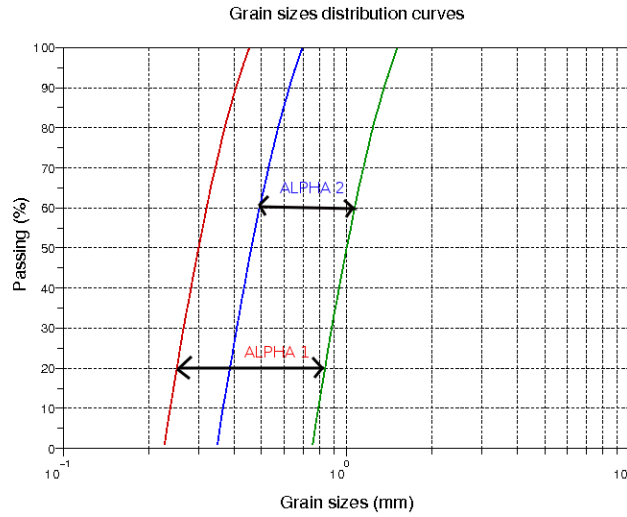
Figure 3.6: Granulometries of the two cube samples and representation of scale factor effects
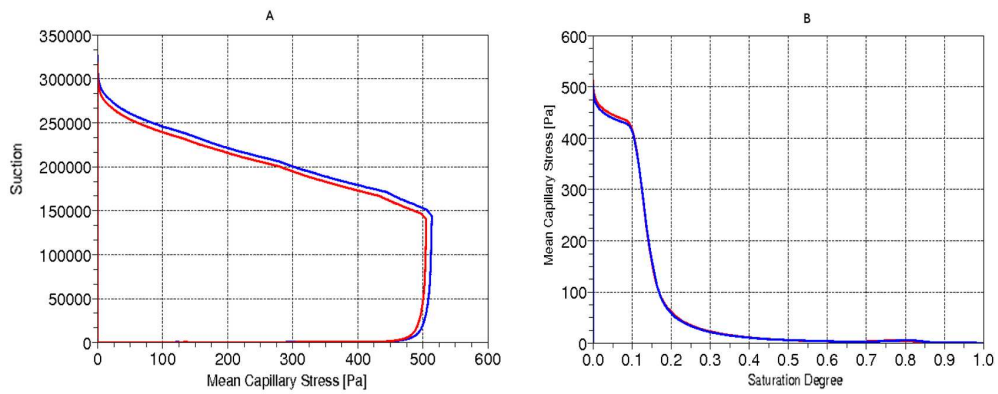

Figure 3.7: Validation of the scale factor effects on computation of capillary forces. A. Mean Capillary Stress vs Suction curve. B. Saturation degree vs. Cohesion curve.
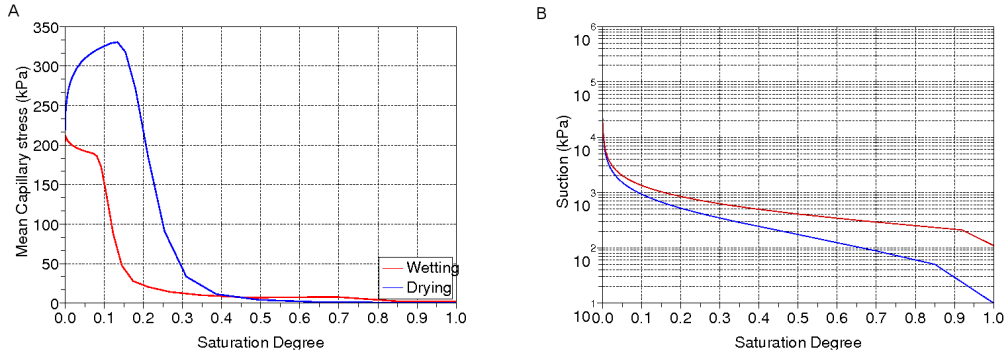
Figure 3.8: Soil-Water Characteristic Curves - Wetting and drying processes

A second session of simulations were performed on a cube, subjected to wetting and drying processes. A very small dimension of simulated grains was adopted here $(3\mu m)$, which can be assimilated to a (fine) lime. The intentions here were to analyse the effects of wetting and drying processes on the evolution of capillary forces and cohesion magnitude. Fig. 3.8 shows the evolution of the suction and of the mean capillary stress during the processes. The resulting curves are classical, not coincident for a given level of suction, because of the hysteretic process implemented in the code. For the drying process, the sample is saturated and fusioned meniscii are initially everywhere between the grains. The decrease in water content is simulated by increasing the capillary pressure, resulting in an increase in cohesion, until the disappearance of menisci due to high suction values (see 3.8b). For the wetting process, meniscii are initially present only between contacting grains. Subjected to a wetting process, decreasing Δu, the sample exhibits a fewer cohesion compare to the drying path, due to a lower number of activated menisci.

3.3 Slope stability

In this last section the effects of water menisci between grains is evaluated through a slope stability analysis. Based on the work of Griffiths and Lu [10], where the effects of rising water table in a silty slope were investigated through simulations performed discretizing the slope in elastoplastic finite elemnts (see fig.3.9), an infiltration induced water content increase, is numerically simulated by rising the water table level at each iteration, imposing the distribution profile of the matric suction. As introduced in 3.1 a linear hydrostatic profile of the matric suction is considered, being a choice that
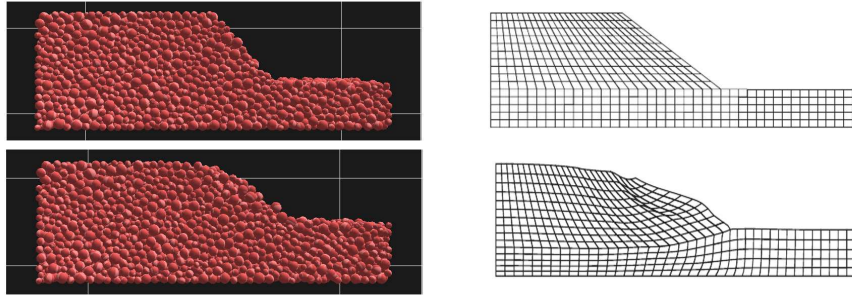
Figure 3.9: On the left, the discrete element model used in this work. On the right the finite element model by Griffiths and Lu [10]
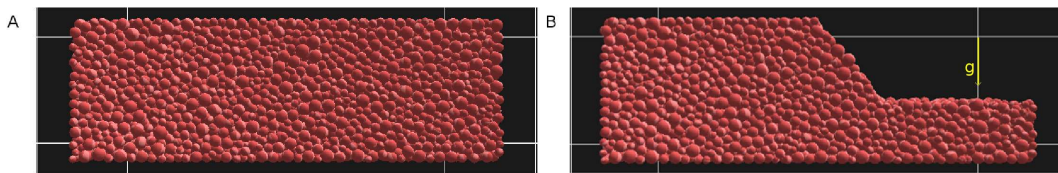

Figure 3.10: Phases of preparation of the slope model

conciles simplicity and conceptual intentions. The aim of the work is to numerically reproduce the forces effectively acting in a granular soil, searching the equilibrium between the gravity effects, which are obviously dominant in dry media, and the capillary effects, whose beneficent effects on stability are dependent on the matric suction magnitude and on the dimension of the grains. Instabilities due to a variation of those quantities, inside a simulated slope, are investigated. This consists solely in matric suction variations, which are often the cause of slope instabilities in real geotechnical problems [1].

3.3.1 Stability in dry conditions

A first simulation was performed for a dry slope whose geometry was defined as input. Thecreation process of the slope model can be described in two different phases (fig.3.10): 1) A parallelepipedic sample is created and compacted, following the same process described for the preparation of the dense sample for triaxial tests (see 3.2.3); 2) The simplified geometry of a slope is recovered by excluding a number of spheres through geometrical conditions, and the gravity is applied on each particle. An inclination of 50 was set, considering that choice useful to obtain a sensible readjustment of the slope to a stable configuration. A function is available in YADE (*Body State*), that
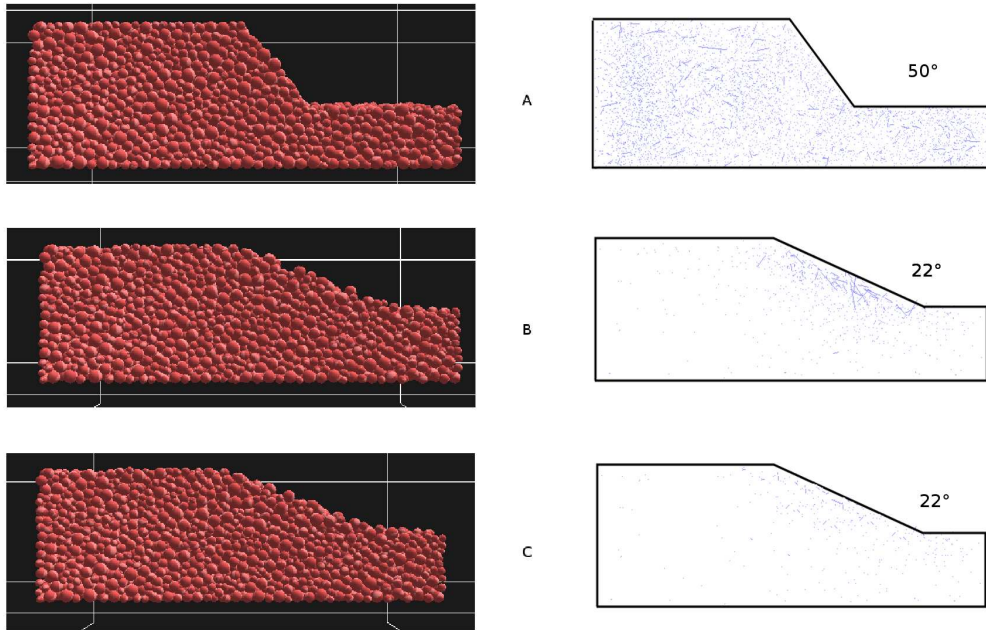
Figure 3.11: Slope stability analysis in dry conditions - Evolution of the slope geometry (left) - Accelerations and velocities fields (right) - A. Initial configuration (0 iterations). B. 25000 iterations. C. 50000 iterations

allows the representation of velocities and accelerations for each sphere, by vectors of proportional magnitude and correspondent direction. Fig. 3.11 shows three phases of the stabilization process of the slope. The top images refers to the initial configuration (A), any movement is optically remarquable, but almost each particle of the slope is characterized in this phase by a significant value in velocity and acceleration. After 25000 iterations (B), the slope reaches almost completely its readjustment. It is clearly remarquable the gravity-induced motion of particles to a more stable configuration, which is completely reached after 35000 iterations. The $UnbalancedForce$ is considered as an indicator for the quasi-static equilibrium, as it has been defined in 3.2.1. Here the same criterion is used, and fig. 3.12 shows its evolution over the stabilization process. It is worth noticing how the final configuration for the slope is characterized by an inclination of the slope equal to approx. 22°, corresponding to the residual friction angle which came out from dry triaxial tests performed on samples of the simulated material (see 3.2.3) The analysis of the stabilization process which characterize a dry granular slope, from an initial defined configuration to the final stable, "quasi-static" configuration, is fundamental in order to evaluate the effects of the cohesion resulting from
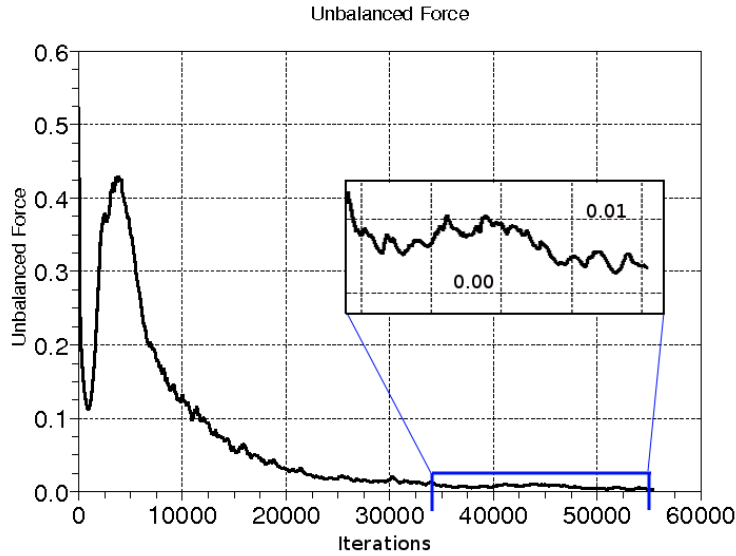
Figure 3.12: Simulation of a dry slope stabilization - Evolution of the unbalanced force versus the number of iterations

the presence of water in the soil.

3.3.2 Stability in wet conditions

Slope stability analysis in wet conditions are presented in this section. In soil strata characterized by low saturation degrees ($Sr < 25\%$), the presence of water as a discontinous phase results in local attractive capillary forces and, macroscopically, in a positive contribution cohesion for the stability of the medium. A linear hydrostatic profile for the matric suction was set. As presented previously, the scale factor α (see 3.2.1) allows the simulation of different materials, being defined as the ratio between the characteristic dimension of the real material and the average dimension of particles used in the numerical simulations. The stabilization process and the effects of the water table rising can be described as follows:

- A profile of matric suction is defined for the slope, setting a depth for the water table level. Menisci between couples of grains are so created, whose effects in terms of capillary forces and resultant cohesion (evaluated as the mean capillary stress, see 2.5) depend on the local value of capillary pressure. The slope is then allowed to stabilize under these conditions;

34

- The water table level is rising up at each iteration with a constant step, up to the saturated condition for the slope. This results in a change of matric suction, whose effects evaluation constitute one of the scopes of this work.

Sand slope analysis

In a first session of simulations, the behaviour of a sand was modelled. An average dimension of the grain had been taken equal to 1mm, the correspondent scale factor was therefore computed equal to 0.286. The initial water table level was chosen considering the results of the wetting and drying processes performed on a sample of *sandy* material (3.2.4). The maximum value of tha mean capillary stress is obtained for values of matric suction ranging approximately between 50000 Pa and 100000 Pa. The water table position was then set at a depth of x meters under the ground surface to obtain the maximum contribution in terms of cohesion along the slope profile (see fig.3.14). In tab. 3.3.2 the parameters used for the simulation are resumed. The slope

$\Phi_{sand,av}$	$\Phi_{slope,av}$	Scale Factor	W.t. depth	Dimensions of the sample
$[m]$	$[m]$	$[-]$	$[m]$	$[m]$
0.001	0.35	$2.86 \cdot 10^{-3}$	50	150x50x50

Table 3.3: Parameters used for the *SlopeStability* simulation on a sandy slope

was then left to reach the stability before rising up the water table. The quasi-stable configuration is reached more rapidly (27000 iterations) than in the dry case, which was predictable, considering the attractive effect of the capillary pressure. However, the contribution in cohesion is less important than the gravity effects. In fig.3.13, the left coloumn represents the different phases of the simulation, as optically remarquable through the YADE graphical tools. The slope, initially prepared as shown in (3.13A), seems to reach a quasi-stable configuration (3.13B) and to not undergo under any shockly instability up to the end of the wetting process (3.13C). The velocity field, represented on the right coloumn, confirm all the optical evidences. At the initial configuration (A), all the particles are interested by a non-zero velocity, which is reasonable considering the introduction of the gravity and capillary pressure to act on each particle. After the stabilization process and further, during the water table level rising, a feeble motion is detected at the slope surface, which does not result in any significative evolution. Fig. 3.14A represents the profile of matric suction along the slope height (relative) at
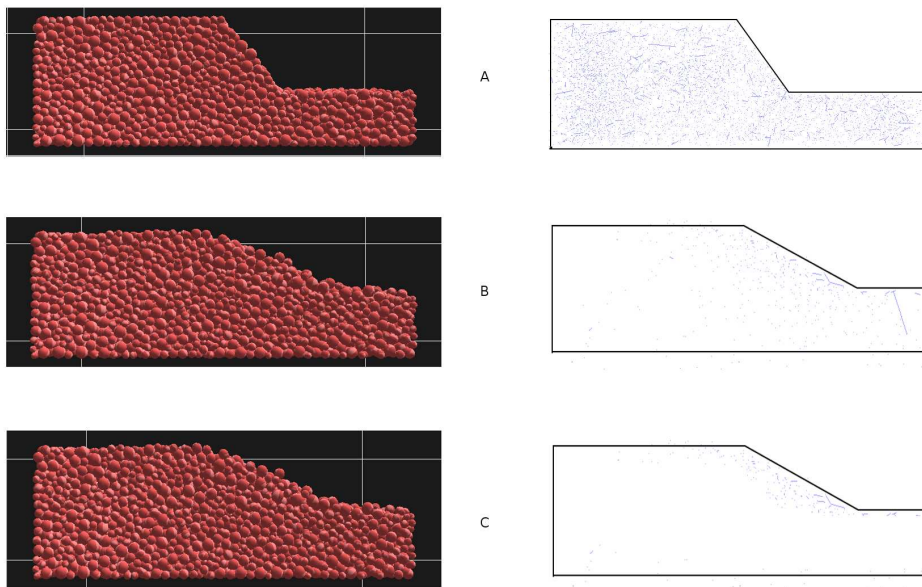
Figure 3.13: Simulation of instabilities due to wetting processes for a sandy slope - Front side view of the slope model (left). Velocity field (right) - A) 0 iterations. B) 25000 iterations (stable). C) 125000 iterations (saturated)
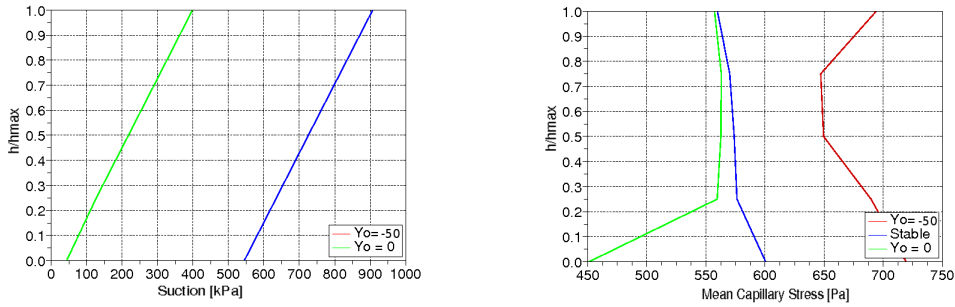
Figure 3.14: A. Profile of matric suction (A) along the slope profile (sand) and mean capillary stress profile and evolution (B) during the water table level rising

the initial configuration and at half wetting process, when the water table level stays at the base of the slope. The contribution in terms of cohesion, evaluated through the value of mean capillary stress, varies between 600Pa and 700Pa, along the soil height (see fig.3.14B), and reduces as a consequence of the water table rising. Values of cohesion in such these ranges do not produce an appreciable contrast to the tendency of particle to fall under the effects of the gravity acceleration. The weak effects of the water table rising are remarquable in fig.3.15A, where the evolution of the $UnbalancedForce$ after the stabilization process ($Unb.F. < 0.01$) is plotted. It is interested by strong ripples but never increase significatively, as a consequence of the unforceful importance of the capillary effects for the grain size considered. The evolution of the kinematic energy, during the wetting process, is plotted (see fig.3.15B) for a streap of slope of thickness equale to h/6, considered at approximately half of the total height. All seems to confirm what was optically remarquable, a variation in kinematic energy is detected, but within very low values to be sufficiently significative.

Silt slope analysis

In a second session simulations a smaller average dimension of the grains is considered, expecting that capillary and gravity effects would be comparable, realizing a condition of quasi-staticity for the slope. A mean radius of $3\mu m$ is considered, assimilating the material to a fine silt. The profile of matric suction is defined in order to ensure an appropriate contribution of cohesion for the stability (fig.3.16). Considering the wetting and drying tests performed on a silt sample (see fig. 3.8), the matric suction is set to a range between 5MPa and 10MPa at the initial configuration and during the stabilization
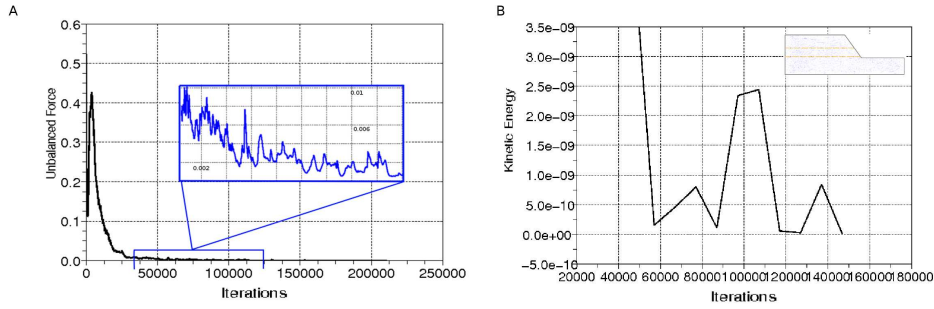
Figure 3.15: A. Evolution of the *UnbalancedForce* during the simulation (sand) B. Kinematic energy evolution of a streap of slope during the water table level rising

process (see fig.3.16). In tab. 3.3.2 the parameters used for the simulation are resumed. In fig.3.17 it can be seen how the cohesion plays an important

$\Phi_{silt,av}$	$\Phi_{slope,av}$	Scale Factor	W.t. depth	Dimensions of the sample
$[m]$	$[m]$	$[-]$	$[m]$	$[m]$
$3 \cdot 10^{-6}$	0.35	$8.6 \cdot 10^{-6}$	-50	150x50x50

Table 3.4: Parameters used for the *SlopeStability* simulation on a sandy slope

role, realizing a sufficient attractive force between the particles of the slope, during stabilization phase. Differences from the dry or the sand case are optically remarquable, the beneficient effects of the water bridges existence between fine grains is obviously confirmed also by a numerical indicator, the number of iterations to reach the stability, the lowest with respect with the other cases studied, being around the 13000 iterations. The rise of the water table results in the annulation of the contributions of cohesion to the stability and the consequent motion of the slope, whose volume deformations and shear strength are carried by the only solid phase, as described in Terzaghi (1.4) and seen for the dry case. Considering the new state conditions, the slope seems to reach a new quasi-stable configuration (D). The velocity field, represented in fig.3.17 for four different phases, confirms the considerations done on instabilities caused by the rising water table in the slope. The soil particles, bonded at the initial configuration by liquid bridges resulting from capillary effects, result to be in motion during the wetting process (C-D) and the gradually annulation of the capillary forces. A surface instability is detected at the last phase (D), up to the saturated conditions. The evolution of

38

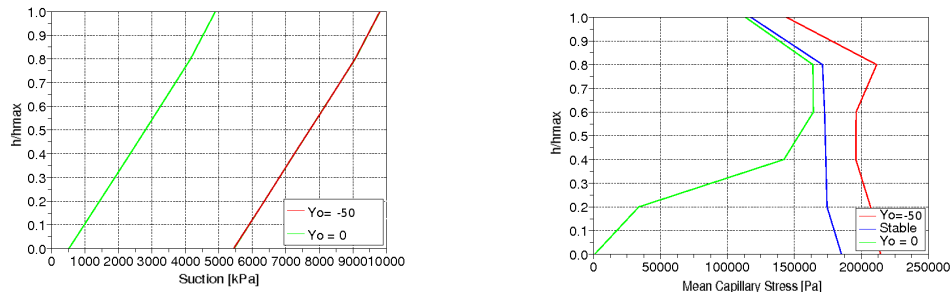Figure 3.16: A. Profile of matric suction (A) along the slope profile (silt) and mean capillary stress profile and evolution (B) during the water table level rising
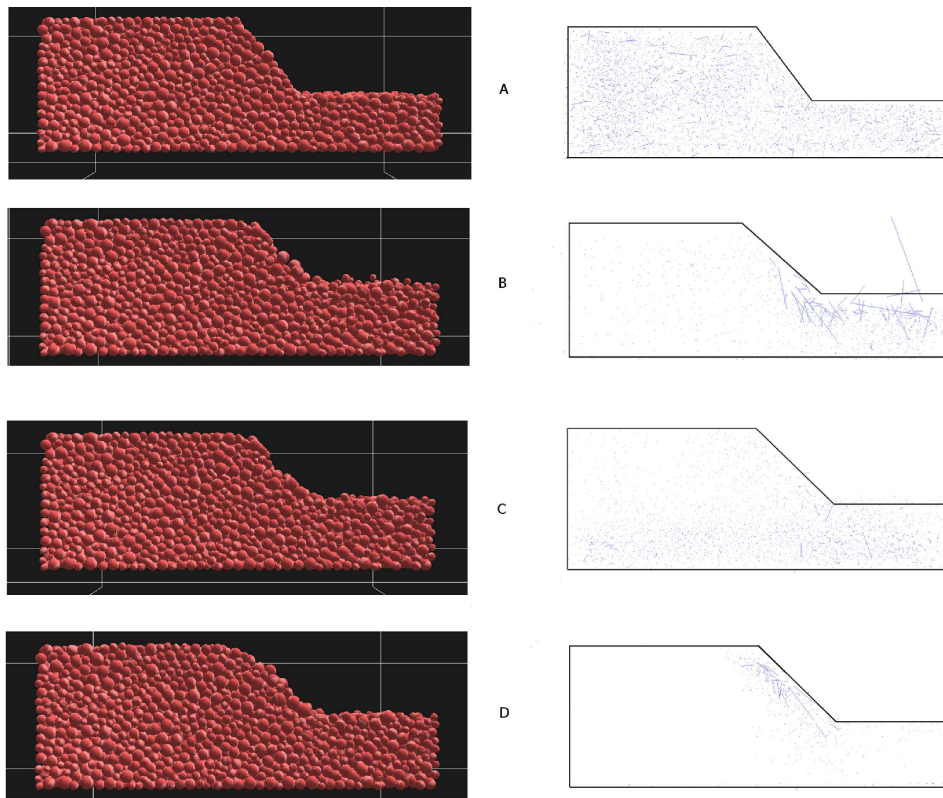

Figure 3.17: Simulation of instabilities due to wetting processes for a silty slope - Front side view of the slope model (left). Velocity field (right) - A) 0 iterations. B) 25000 iterations (stable). C) 75000 iterations D) 125000 iterations (saturated)
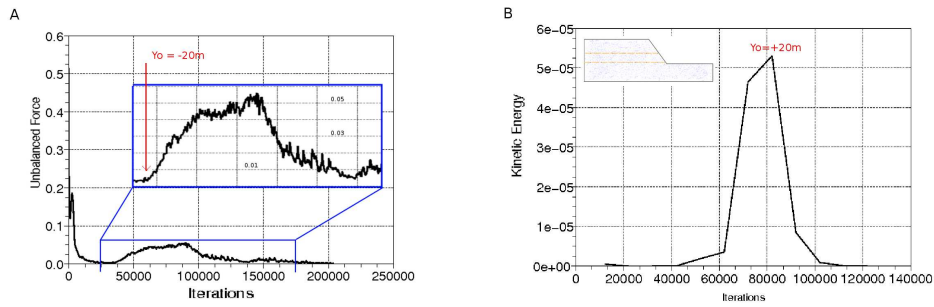
39

Figure 3.18: A. Evolution of the *UnbalancedForce* during the simulation (silt) B. Kinematic energy evolution of a streap of slope during the water table level rising

the unbalanced force versus the number of iterations (see fig.3.18A) constitutes an important confirmation of the instabilities due to the elevation of the water table. Once the wetting process starts, the unbalanced force increases noticeably as a result of the gradual annulation of the cohesion contribution inside the medium. The triggering of the motion is detected to occur around 40000 iterations, the water table being 20 meters below the base of the slope. The evolution of the kinetic energy for the same streap was also considered for the sand. As expected, it shows a more significant variation for the silty case (see fig.3.18B) than in the sandy one. A peak is detected, around 80000 iterations, corresponding to a water table located 20 meters above the base of the slope.

CONCLUSIONS

The model seems to be able to take into account the cohesive contribution of capillary effects in subsurface unsaturated soils, resulting from the liquid bridges bonding of the grains. Stability simulations were performed on a schematized geometry of slope, providing the characterization of the simulated material and the validation of the correct action of a scale factor, introduced to make the model able to simulate the behaviour of any granular material.

The mechanical properties of the simulated material are evaluated through triaxial tests performed on dry samples, opportunely prepared to ensure two different states of packing, a loose and a dense one. Classical results are obtained, in terms of axial and volumetric strain evolutions for increasing level of compression stress. Both the stress-strain curve and the evolution of porosity converge at the critical state to a unique value, assuring the same material is dealing with.

The introduction of a scale factor to simulate real granular materials, provided a characteristic dimension of the grains, allows the simulation of wetting-induced instabilities for a sand and a silt slope. The soil-water characteristic curves are recovered for these two materials. In order to evaluate the relation between the matric suction and the correspondent value of the mean capillary stress, a stress quantity is adopted to quantify the cohesion contribution due to capillary effects. This allows the definition of a suction profile, during the *SlopeStability* simulations, ensuring the maximum capillary contribution in cohesion along the slope height.

A linear profile for the matric suction above the water table is chosen for the sake of simplicity, the suction profile in natural conditions being more complex, resulting from environmental phenomena and from the slope hydric history. Anyway, considering the aim of the work, simulating the water content increase by rising the water table level, appears to be an acceptable assumption to appreciate such a condition of stability, gravity and capillary effects, acting simultaneously on particles, and evolving beacuse of the saturation conditions of the material. Results from simulations on wet slopes have been compared to the pilot dry case.

The simulation of the sandy granular slope has shown how the capillar contribution to cohesion, evaluated through the computation of the mean capillary stress, is too low compared with the gravity effects on the particles. The slope has reached the quasi-stable configuration in a less number of iterations than in the dry case, and the evolution of the stability indicator has been characterized by strong ripples, but never reaches values over the

limit expressing the quasi-static evolution.

It is not the case for the silty slope, where the effects of water play an important role for its stability. Differences from the dry case have been optically remarqued and the stability configuration has been reached in two times less time than the case of sand. Thanks to the contribution in cohesion provided by the water menisci between grains, the higher values of capillary stress along the slope height seem to be comparable with the gravity effects on soil particles. The effects of rising the water table can be noticed optically, since a new stable configuration is reached as a consequence of the annulation of the capillary forces, and numerically, since the evolution of the stability indicator shows a clear increase during the water table rising, up to finally return below the quasi-staticity limit.

The interpretation of the micromechanical mechanisms which take place in the pendular regime of unsaturated soils, results finally in a suitable model to consider the effects of increasing the water content on the stability of a granular material. It is worth noticing that no dynamic effects are taken into account in this work, whose main scope was the description of the conditions of triggering collapse of partially saturated slopes. The real *phenomenology* of the collapse phenomenon would need some other description of dynamical origin that are not considered here.

Bibliography

[1] D.G. Fredlund and H. Rahardjo. Soil Mechanics for Unsaturated soils. *Wiley-Interscience Publ.* 2003;

[2] L. Scholtés, P.-Y. Hicher, F. Nicot, B. Chareyre, F. Darve. On the capillary stress tensor in unsaturated granular materials *Submitted to Int. J. Eng. Science* 2007;

[3] L. Scholtés, B. Chareyre, F. Nicot, F. Darve Micromechanics of granular materials with capillary effects. *Submitted to Int. J. Eng. Sc.* 2008;

[4] B. Chareyre Modelisation du comportement d'ouvrages composites sols-geosynthetique par lements discrets Application aux ancrages en tranches en tete de talus. *PhD Thesis - Universit Grenoble I* 2003;

[5] P.A. Cundall and O.D.L. Strack. A discrete numerical model for granular assemblies. *Géotechnique* 1979; **29**(1):47–65.

[6] F.Donzé and S.A.Magnier. Formulation of a three-dimensional numerical model of brittle behaviour. *Geophys. J. Int.* 1995; **122**:790–802.

[7] M. Barla and M. Castelli Metodi di analisi di stabilit dei versanti *XI ciclo di conferenze di meccanica e ingegneria delle rocce* 2006; **63**–84.

[8] M. Nuth and L. Laloui. Effective stress concept in unsaturated soils: Clarification and validation of a unified network. *Int. J. Numer. Anal. Meth. Geomech.* 2007;

[9] F. Nicot, F. Darve. A multi-scale approach to granular materials. *Mechanics of Material* 2004; **37**:980–1006.

[10] D.V. Griffiths and N. Lu. Unsaturated slope stability with steady infiltration or evaporation using elasto-plastic finite elements *Int. J. Numer. Anal. Meth. Geomech.* 2005; **29**:249–267.

[11] S.H. Liu and D.A. Sun. Simulating the collapse of unsaturated soil by DEM *Int. J. Numer. Anal. Meth. Geomech.* 2002; **26**:633–646.

[12] M.J. Jiang, S. Leroueil, J.M.Konrad. Inisght into shear strenght functions of unsaturated granulates by DEM analyses *Computers and Geotechnics* 2004; **31**:473–489.

[13] N. Lu and D.V. Griffiths Profiles of steady-state suction stress in unsaturated soils *J. Geotech. Geoenvir. Eng.* 2004; **10**:1063–1076.

[14] J.M. Gasmo, H. Rahardjo, E.C. Leong Infiltration effects of a residual soil slope *Computers and Geotechnics* 2000; **26**:145–165.

[15] J. Kozicki, F.V. Donzé. A new open-source software developed for numerical simulation using discrete modelling methods *Comp. Meth. Appl. Mech. Eng. (accepted for publication)* 2008;

[16] YADE open-source GNU-GPL software.http://yade.wikia.com/wiki/Yade.

Europass Curriculum Vitae

Personal information

First name(s) / Surname(s)	**Emanuele Catalano**
Address(es)	130, Via Filadelfia – 10137 Torino - Italy
Telephone(s)	+393472662478 Mobile: +33620415843
E-mail	ema.catalano@gmail.com
Nationality	Italian
Date of birth	15/06/83
Gender	Male

Education and training

Dates	2002-2006
Title of qualification awarded	Bachelor's degree in civil engineering
Principal subjects/occupational skills covered	Civil geotechnical engineering
Name and type of organisation providing education and training	Politecnico di Torino , I faculty of engineering
Level in national or international classification	96/110

Education and training

Dates	1997 - 2002
Title of qualification awarded	High School Diploma
Principal subjects/occupational skills covered	Scientific – Informatic course
Name and type of organisation providing education and training	Scientific Liceum "N. Copernico" - Torino
Level in national or international classification	83/100

Work experience

Dates	March 2007 – April 2007
Occupation or position held	Stage

Main activities and responsibilities	Capitalisation of anti-erosion works of a hydrologic basin in the province of Ioba, Burkina Faso
Name and address of employer	ONG CISV « Comunità internazionale servizio volontariato » , Torino
Type of business or sector	International Cooperation

Personal skills and competences

Mother tongue(s)	**Italian**

Other language(s)

English, French

Self-assessment

European level (*)

	Understanding			Speaking				Writing	
	Listening		Reading		Spoken interaction		Spoken production		
English	B1	Intermediate	C2	Advanced	B1	Intermediate	C2	Advanced	C2	Advanced
French	C2	Advanced	C2	Advanced	C2	Advanced	C2	Advanced	C2	Advanced

(*) Common European Framework of Reference for Languages

Social skills and competences	Ability to work in group or alone.
Computer skills and competences	Windows and Linux Operative Systems. Programming softwares: Matlab Programming languages: C++, Visual Basic, Pascal Office softwares Graphic softwares: Autocad